

Supplementary Data

Nanoscale Co-Based Catalysts for Low-Temperature CO Oxidation

Xi Wang, Wei Zhong, and Yingwei Li*

School of Chemistry and Chemical Engineering, South China University of Technology,
Guangzhou 510640, China.

* To whom correspondence should be addressed. E-mail: liyw@scut.edu.cn

This PDF file includes:

Figs. S1 to S8

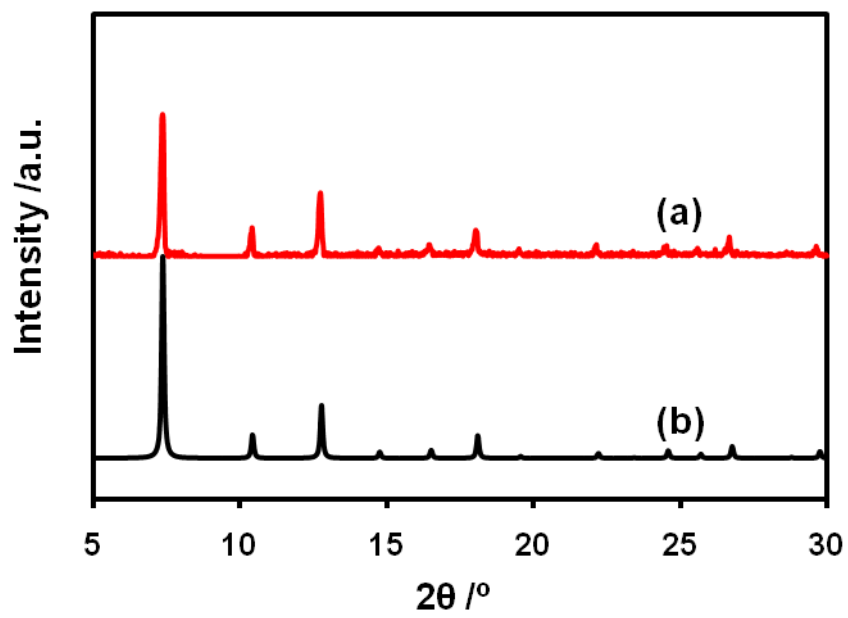


Figure S1. Powder XRD patterns of ZIF-67: (a) as-synthesized, and (b) simulated.

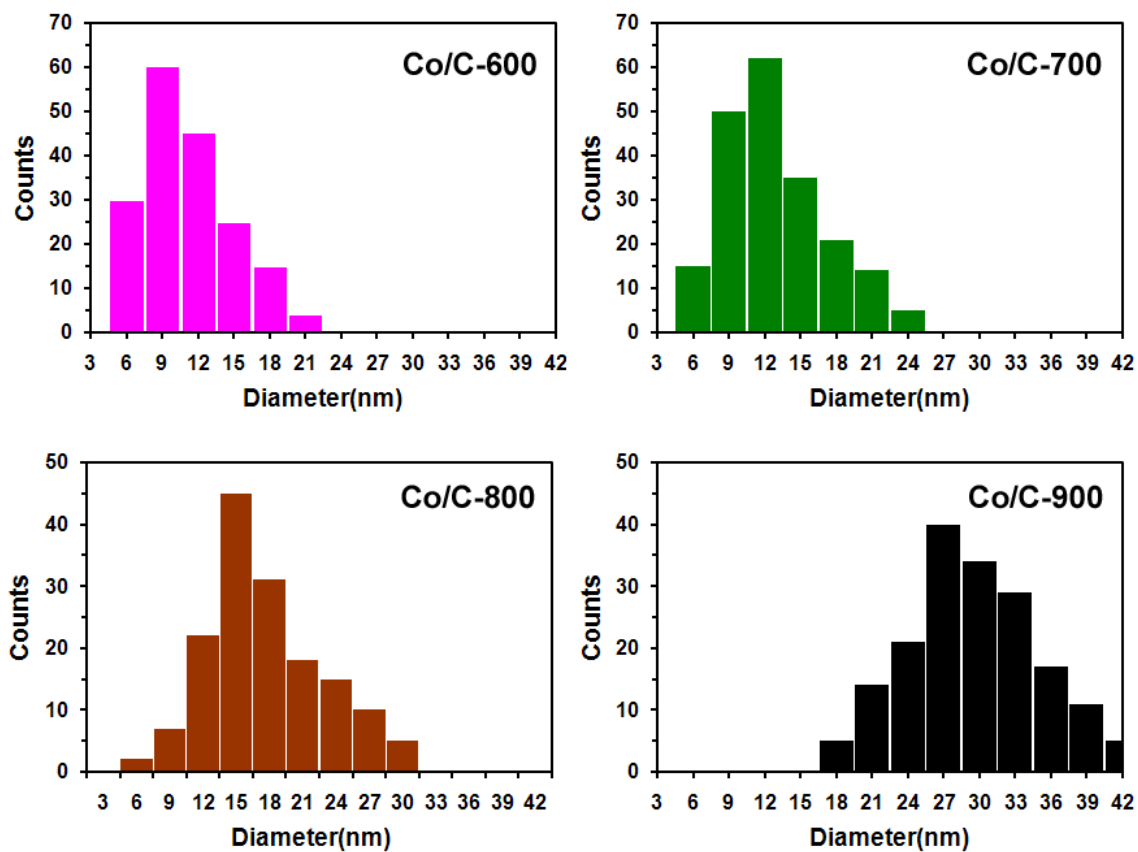


Figure S2. Size distribution of Co nanoparticles in Co/C-X corresponding to TEM micrographs in Figure 2.

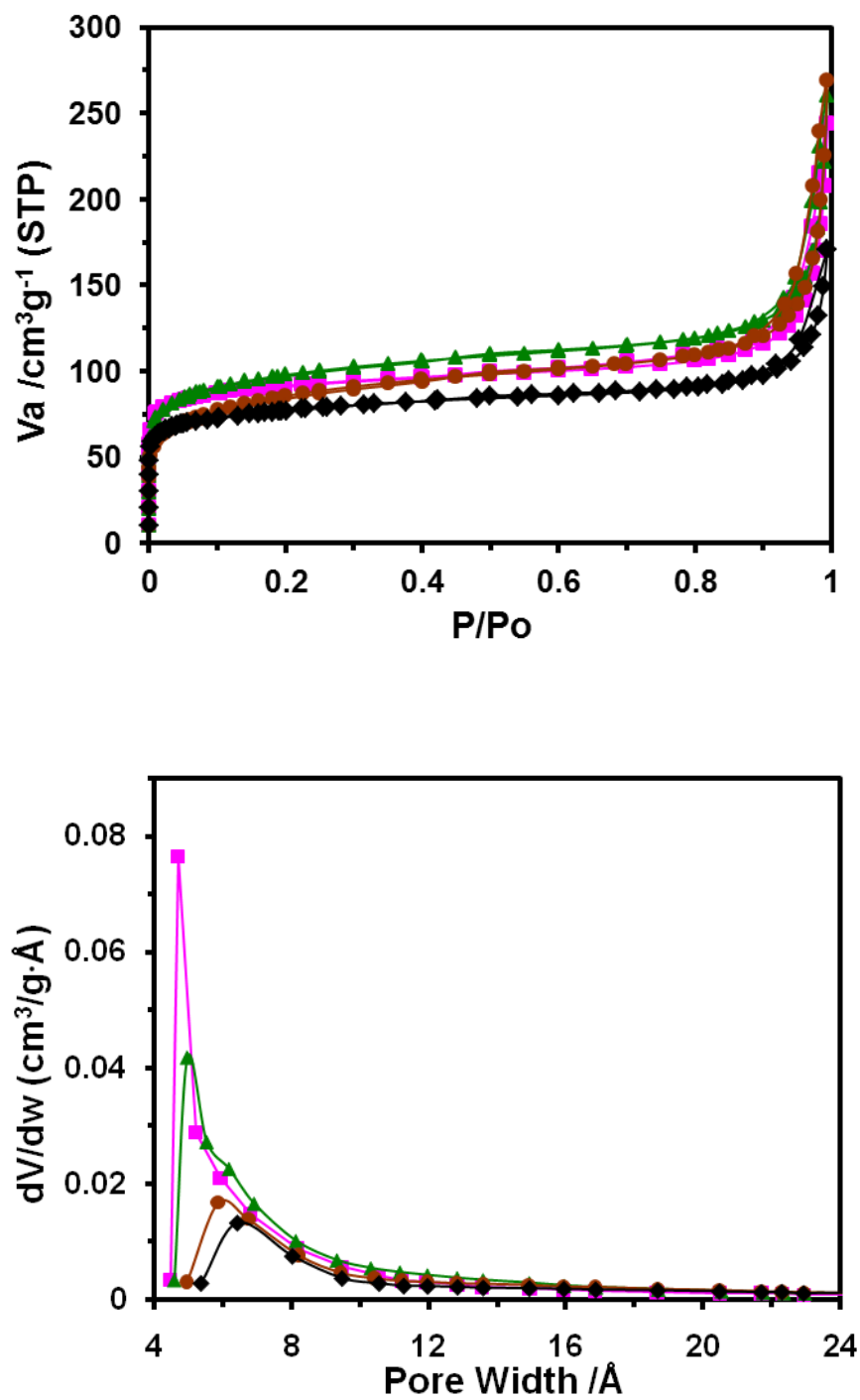


Figure S3. Nitrogen adsorption-desorption isotherms at 77 K (top) and corresponding pore-size distribution curves of Co/C-600 (■), Co/C-700 (▲), Co/C-800 (●), and Co/C-900 (◆).

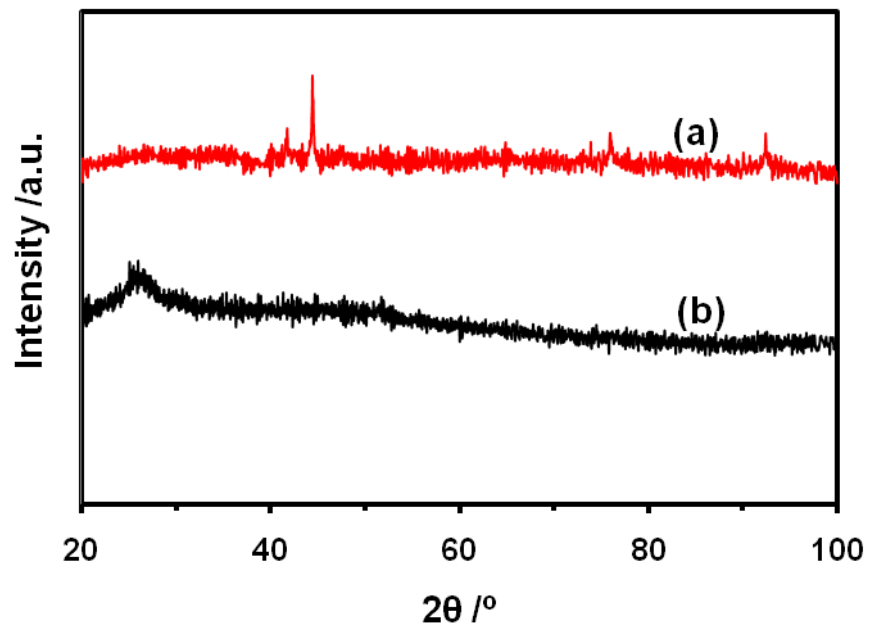


Figure S4. Powder XRD patterns of (a) Co/C-600-Co, and (b) Co/C-600-C.

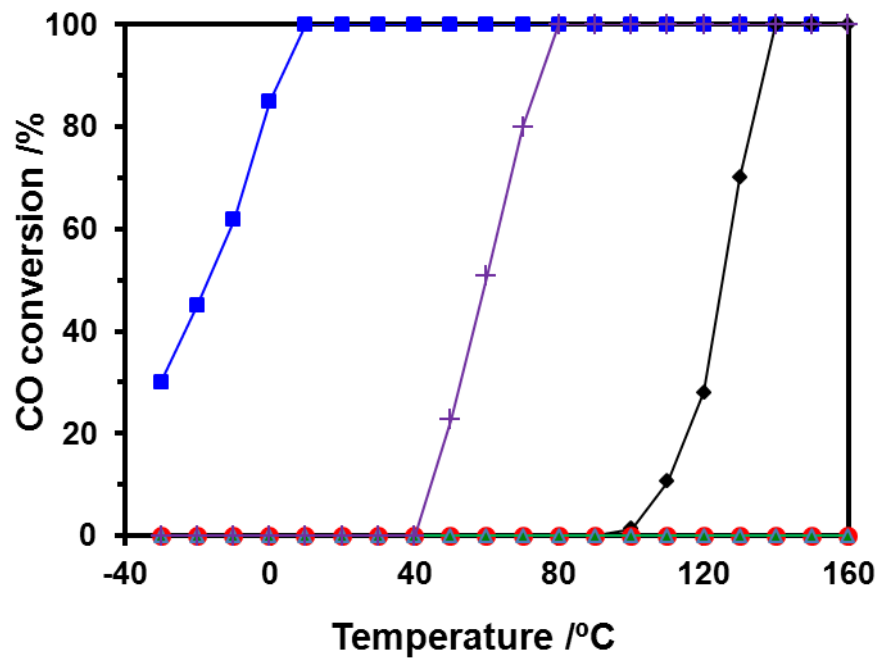


Figure S5. Conversion as a function of reaction temperature for CO oxidation over Co/C-600 (■), Co/C-600-Co (◆), Co/C-600-C (●), Co/AC (+), and Co and AC physical mixture (▲) under dry gas conditions.

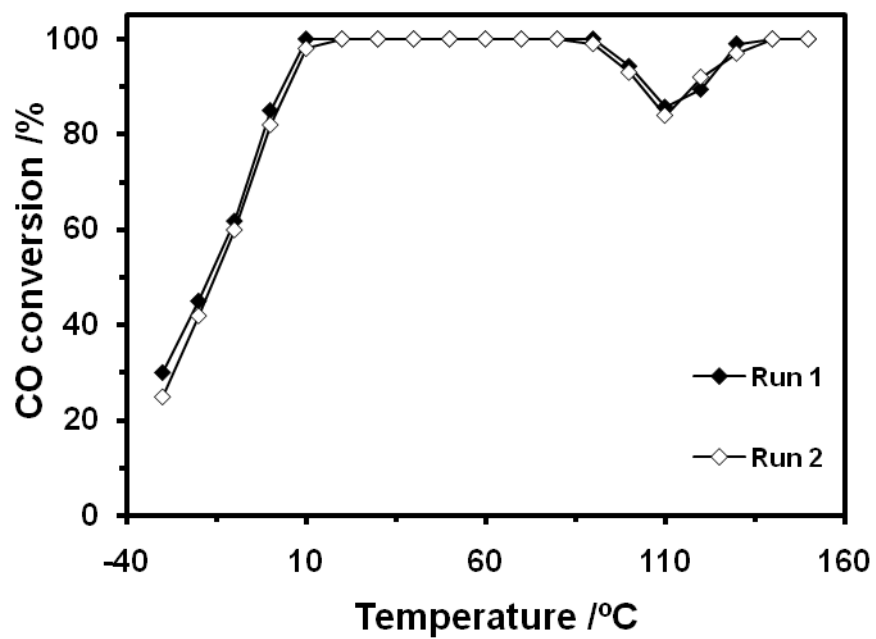


Figure S6. Conversion as a function of reaction temperature for CO oxidation over Co/C-600 under wet gas conditions.

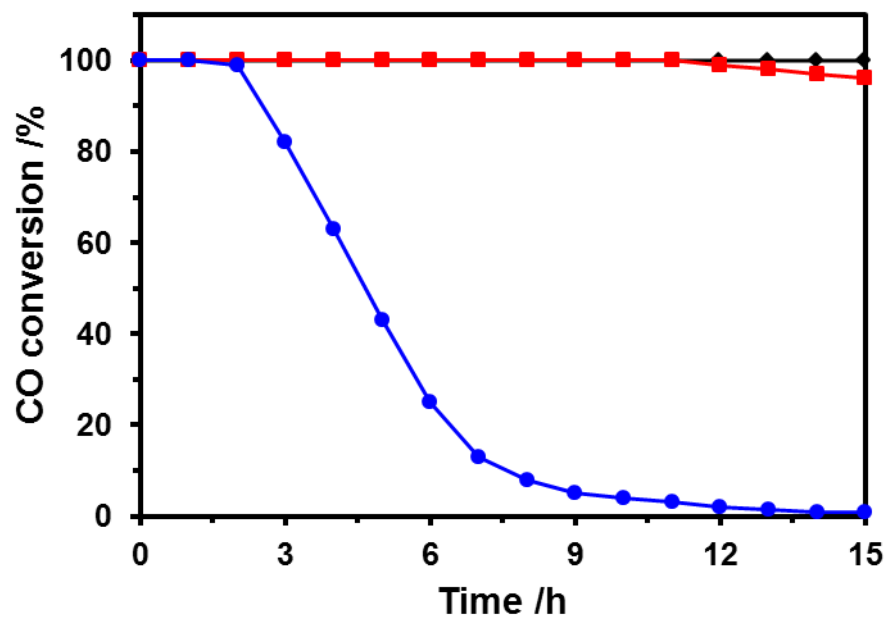


Figure S7. Effect of H₂O concentration on the stability of the Co/C-600 for CO oxidation at a constant temperature of 25 °C for 15 h under 500 ppm moisture (■), 4 vol.% moisture (●), and dry (◆) conditions, respectively.

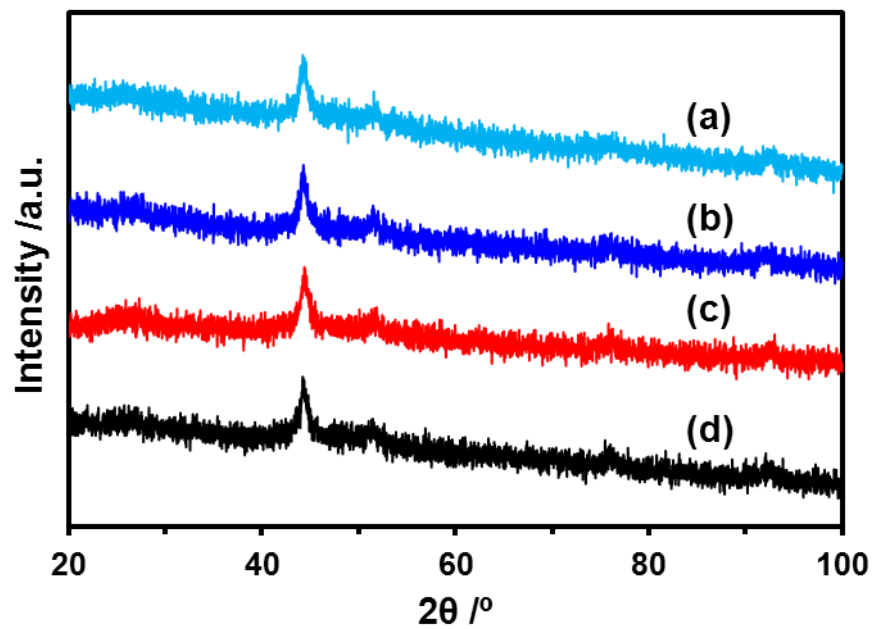


Figure S8. Powder XRD patterns of fresh (a) and used Co/C-600 after the first (b), second (c), and third (d) run of stability test under wet gas conditions corresponding to results in Figure 10.